

A Procedure for Fitting Point Sources in SMEI White-Light Full-Sky Maps



P. Hick[†], A. Buffington and B.V. Jackson

Center for Astrophysics and Space Sciences (UCSD)
email: {pphick, abuffington, bvjackson}@ucsd.edu

Introduction

The Solar Mass Ejection Imager (SMEI)^{2,3} is a full-sky, white-light, CCD-based camera system for observing the inner heliosphere from Earth orbit. SMEI was launched into an 840 km Sun-synchronous terminator orbit on January 6, 2003, on the Coriolis spacecraft. It consists of 3 CCD cameras with fields of view (FOVs) of $60^\circ \times 3^\circ$ that combined sweep a 160° arc of sky, covering the whole sky each spacecraft orbit of 102 min. All 4-s exposures from one orbit combine into a composite photometric white-light full-sky map. Several sources contribute to the total signal: light from planets, stars and galaxies, scattered sunlight from the zodiacal dust cloud⁴, Thomson-scattered sunlight from free electrons in the solar wind, and, especially during times of high geomagnetic activity, auroral light⁵. The primary objective in the SMEI data reduction is to isolate the Thomson-scattering signal. This relates directly to the solar wind density and provides a way to observe the heliospheric response to solar disturbances, such as CMEs. One of the steps needed to achieve the desired photometric precision (0.1% differential photometry per square degree of sky) is to fit and remove point sources (stars and planets) brighter than 6th magnitude from the full-sky maps. Buffington *et al.* (2007)¹ use time series for these fitted stars to calibrate SMEI against the LASCO C3 coronagraph. A catalogue of about 5600 stars with expected magnitudes in the SMEI bandpass, serves as the primary list of point sources, augmented with the brightest planets (Jupiter, Saturn, Venus and Mars). The DE405 ephemeris is used for planetary positions are (E.M. Standish, NASA/JPL).

The Full-Sky PSF

The point spread function (PSF) of the SMEI optics has a highly asymmetric shape^{6,7}, and varies in shape with position in the FOV of each camera¹. A typical sky location transits the FOV at an almost fixed position in the long dimension, crossing the narrow dimension in about one minute. A dozen or more sequential CCD frames contribute to the brightness at that location in the composite skymap, and the PSF is the net average resulting from the superposition of all contributing frames, largely averaging variations of the CCD PSF with position along the narrow dimension. The full-sky PSF still has several unusual properties: it has a width of 1° , is asymmetric, and varies in width depending on where in the FOV the image is formed (Figure 1). Moreover, its orientation on the sky changes over the course of a year.

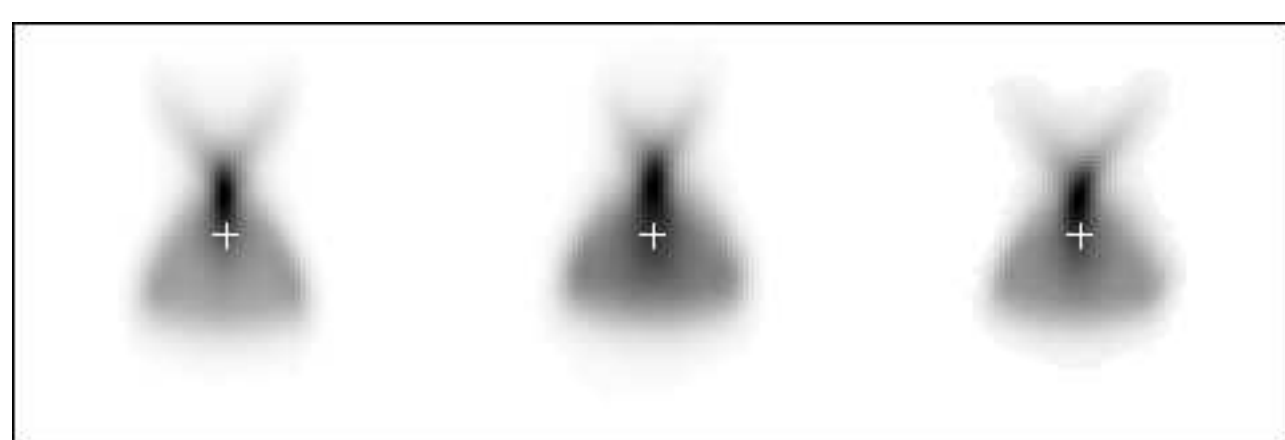


Figure 1: The full-sky PSF for cameras 1, 2 and 3 (left to right) in equirectangular projection. The crosses indicate the centroid. This PSF was determined empirically using stars with no close neighbours. For each camera a 2° square is shown. This "standard star" can be viewed as a star with its centroid at the vernal equinox with $\theta=0$ (see below).

PSF Width and Orientation

The width of the PSF on a CCD frame decreases proportional to $\cos \theta$, where θ is the angle to the optical axis in the long dimension of the FOV. Only the width perpendicular to the PSF symmetry axis (in the θ direction) is affected. In the SMEI skymaps this results in a more narrow PSF when the star is constructed from portions of CCD frames far removed from the optical axis. Since the integrated brightness of a star is conserved, the brightness distribution depends on θ as: $f(\theta, x, y) = \frac{1}{\cos \theta} f(0, \frac{x}{\cos \theta}, y)$

The Coriolis orbital plane maintains a fixed orientation to the Sun-Earth line, resulting in a full 360° rotation relative to the sidereal sky over the course of one year. As a result the FOV, and hence the PSF of each star, changes its orientation on the sidereal sky (Figure 2). The orientation follows from a star's location and known spacecraft attitude.

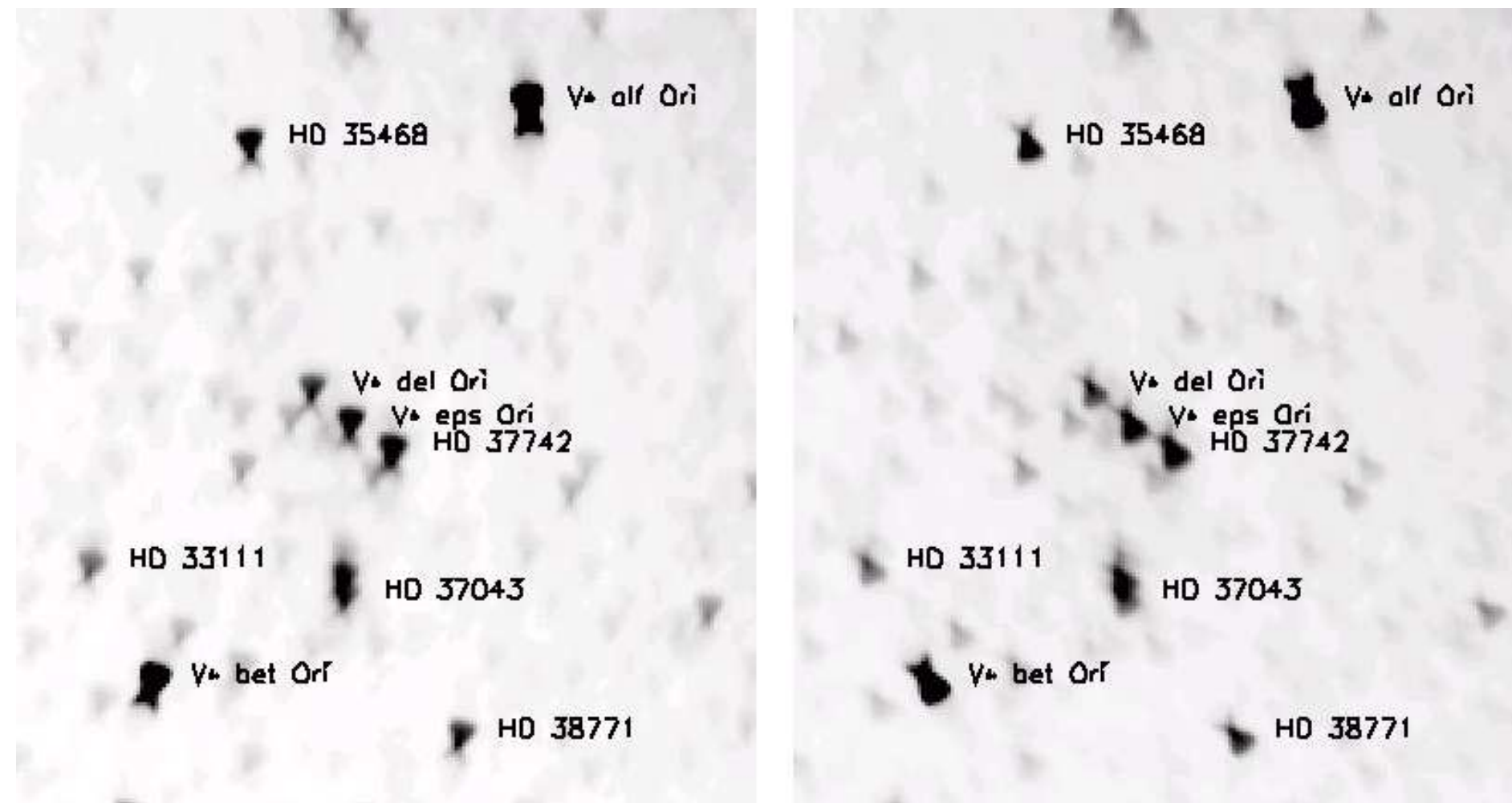


Figure 2: Orion in skymaps for camera 1 (pointing away from the Sun). Left: 2005/11/10 03:25 UT. Right: 2006/01/19 16:37 UT, 2 months later. The greyscale saturates at 1000 ADU¹.

Least-squares fit of point sources

Skymaps are assembled as 3 separate maps with angular resolution of 0.1° , covering the sky using an equatorial reference frame: an equirectangular map ($N \times M = 3600 \times 1200$) covers $|\delta| < 60^\circ$. The polar regions, $|\delta| > 50^\circ$, are covered using a polar projection ($N \times M = 800 \times 800$). Stars are fit and removed in order of increasing magnitude, avoiding complications due to the presence of brighter nearby stars. Where stars brighter than 6th magnitude lie very close together ($< 0.75^\circ$) multiple stars are fit simultaneously. If stars are closer than 0.25° it is no longer possible to separate the PSFs. Only the brighter star is fit (and will include the brightness of the fainter star).

The fit follows a standard least-squares scheme. A box of $5^\circ \times 5^\circ$ (50x50 bins) is selected, centered on the catalogue location of a bright star. For all bins the location, r_{ij} , and sky brightness, f_{ij} , is known. Then

$$f(r_{ij}) = f_{ij} \quad (i \in [1, N], j \in [1, M])$$

where the position is specified in terms of array indices (i, j) into the skymap:

$$r_{ij} = (i, j) \quad (i \in [1, N], j \in [1, M])$$

The centroid is near $i_s = \frac{1}{2}(N+1)$, $j_s = \frac{1}{2}(M+1)$. A star is fitted using a template that consists of a planar sloped background and, for each of the stars fitted simultaneously, a standard star with a scaling factor:

$$f(r_{ij}) = A + a(i - i_s) + b(j - j_s) + \sum_k B_k f^{std}(\bar{r}_{ij}^k)$$

where $f^{std}(\bar{r}_{ij}^k)$ are the brightnesses in the standard star at the equivalent locations \bar{r}_{ij}^k . These are obtained from r_{ij} by applying a sequence of transformations:

- convert from skymap location r_{ij} to equatorial coordinates, *i.e.*, apply the inverse of the map projection, P_M .
- apply a rotation R_{PSF} to account for the PSF orientation.
- apply a rotation R_P to convert from equatorial coordinates near the star centroid to equatorial coordinates near the standard star centroid (at the vernal equinox, $\alpha = \delta = 0$).
- apply a scaling factor $S = \cos^{-1} \theta$ to the right ascension only to account for the variation of the PSF width.
- convert from equatorial to standard star locations, *i.e.*, apply the equirectangular map projection, P_{Std} .

This can be summarized symbolically as:

$$\bar{r}_{ij} = (P_{Std} \times S \times R_P \times R_{PSF} \times P_M^{-1}) r_{ij}$$

The standard brightnesses $f^{std}(\bar{r}_{ij}^k)$ are obtained by linear interpolation in the standard star map at the equivalent locations, and are then multiplied by $\cos^{-1} \theta$ to ensure that the integrated intensity of the star is preserved.

The solution is found using a linear least-squares fit in $2+k$ dimensions (up to $k = 4$ stars are fit simultaneously). The constants A, a, b give the background at the location of the bright star; the constants B_k provide the ratio of the star brightnesses to that of the standard star. In the linear fit each skybin is assigned a weight inversely proportional to the intensity in the full-sky map. This is especially important when fitting bright stars to obtain an accurate fit of the brightness in the background.

In addition to this analytic linear least squares fit several properties of the PSF can be adjusted using a brute-force iterative fitting technique: centroid coordinates, PSF orientation angle, and the PSF widths along and perpendicular to the symmetry axis.

Sidereal Background

Prior to fitting individual stars the unresolved sidereal background (primarily the galactic background) is subtracted (Figure 3). The main motivation is to reduce higher-order derivatives in the underlying background brightness distribution, making it more consistent with the assumption of a planar background. The background map was determined empirically from SMEI full-sky maps.

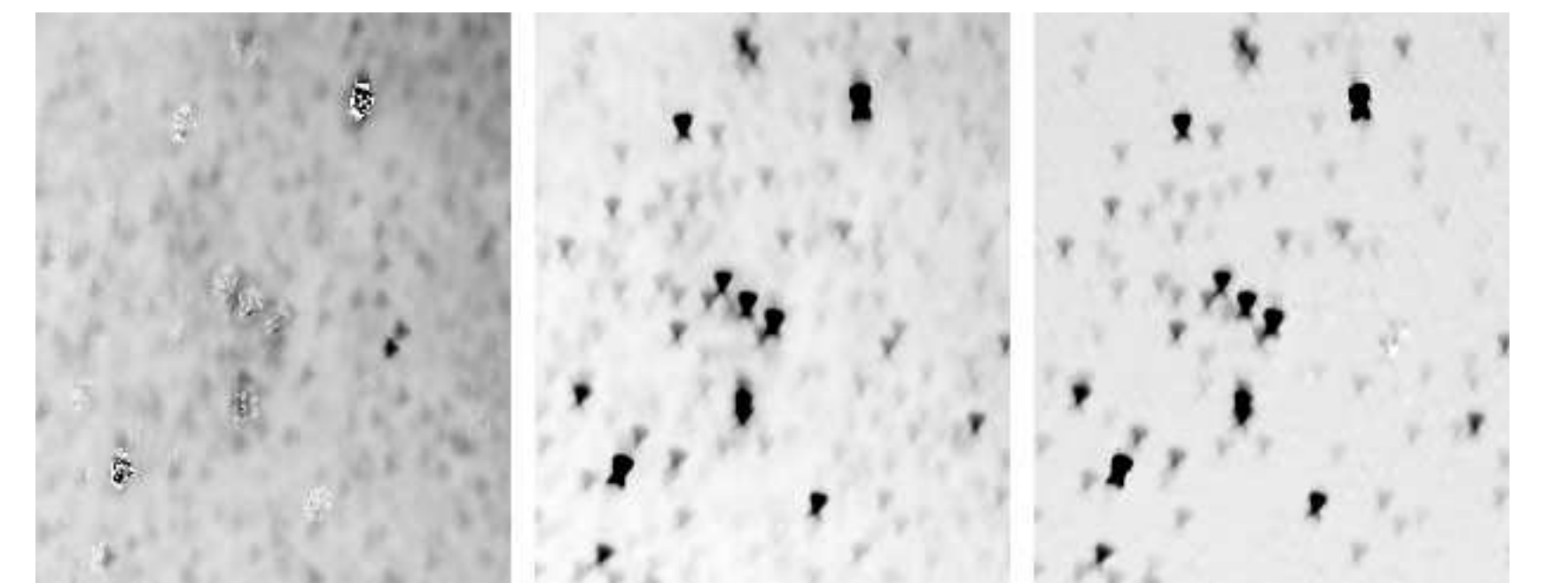


Figure 3: Orion in SMEI skymaps on 2005/11/10 03:25 UT. Left: the unresolved sidereal background. The average is 62 ADUs. Center: the skymap with the average background removed. Right: the skymap with the actual background (left) removed. The greyscale covers 0 to 500 ADUs. The background scale (left) is enhanced by a factor 3 (covers 0 to 167 ADUs).

Results

The section of sky in the constellation Orion contains 149 stars listed in the SMEI star catalogue. Figure 4 shows results for star subtraction using two methods: the basic analytic least squares fit, and a least squares fit with iterative solutions for centroid, PSF width and PSF orientation.

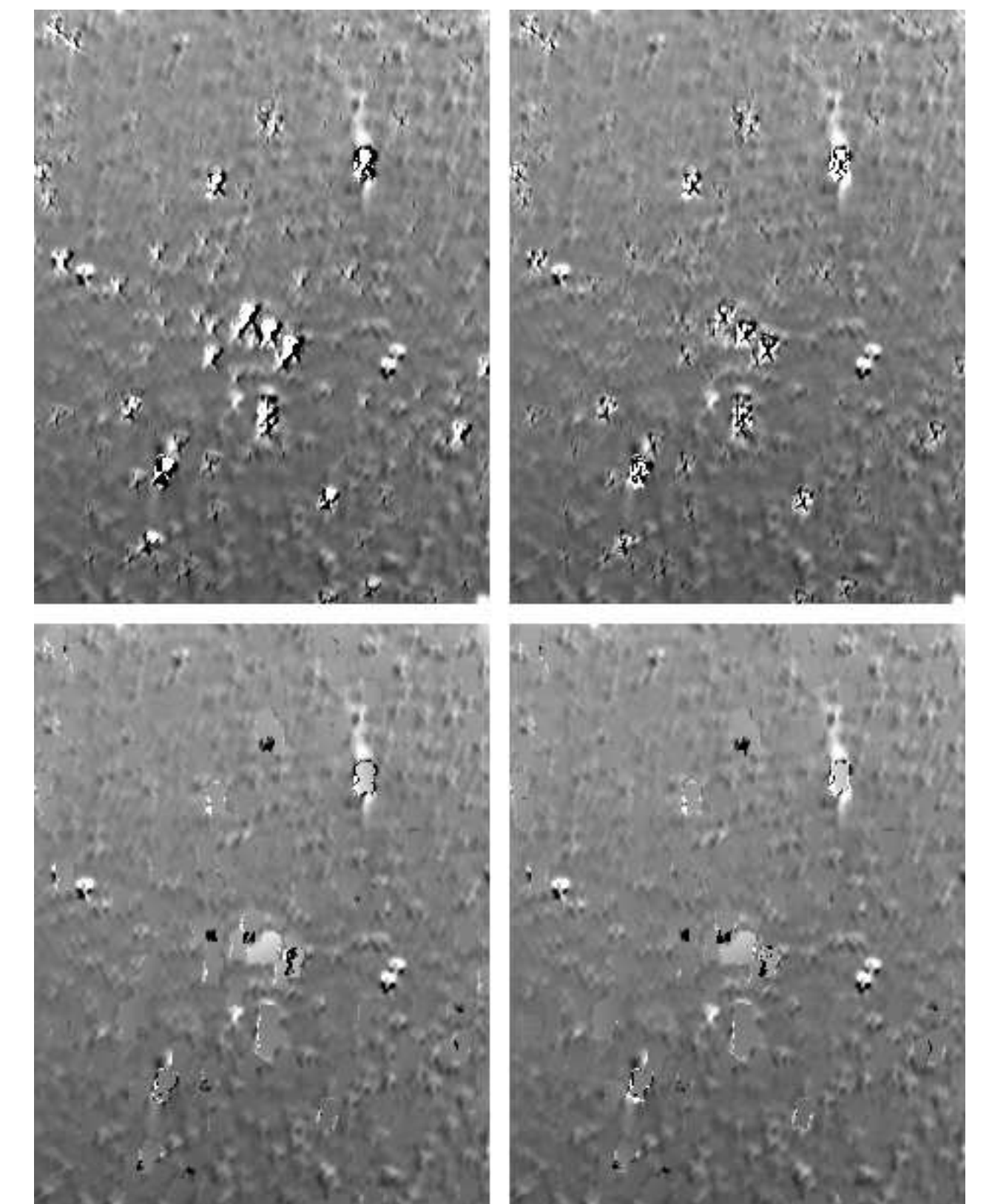


Figure 4: Top-left: subtraction of simple least square fit solution. Top-right: subtraction of least squares fit with iterative solutions for centroid, PSF width and PSF orientation. Bottom: same as top, but instead of subtracting the least squares solution, the PSF is replaced by the planar background solution. The grey scale covers the range 0 (black) to 100 ADUs (white); the average remaining background is about 50 ADUs.

The iterative fit substantially improve the quality of the fit, especially for bright stars. For the brightest stars the standard deviation of the residual decreases: α Ori from 464 to 245 ADU; β Ori from 196 to 124 ADU. A visual inspection confirms this. The three stars in Orions belt are removed more effectively. However, the residuals for a very bright star are still significant, in part because of the inherent noise in the star, but also because of deficiencies in the PSF shape. As an alternative for subtracting the best fit for a star the area within the PSF can be replaced by the fitted planar background. This is guaranteed to remove the inherent noise in the bright star, at the expense of losing information of variations in the background brightness on spatial scales of the PSF. The result of this procedure is shown in the bottom two maps for both least square fits. The difference between the two maps is minimal. For most of the heliospheric solar wind studies done with SMEI observations, involving large scale structures such as CMEs that usually cover many square degrees of sky, these maps are probably sufficient.